



# Fe<sub>3</sub>O<sub>4</sub>@PSC nanoparticle clusters with enhanced magnetic properties prepared by alternating-current magnetic field assisted co-precipitation



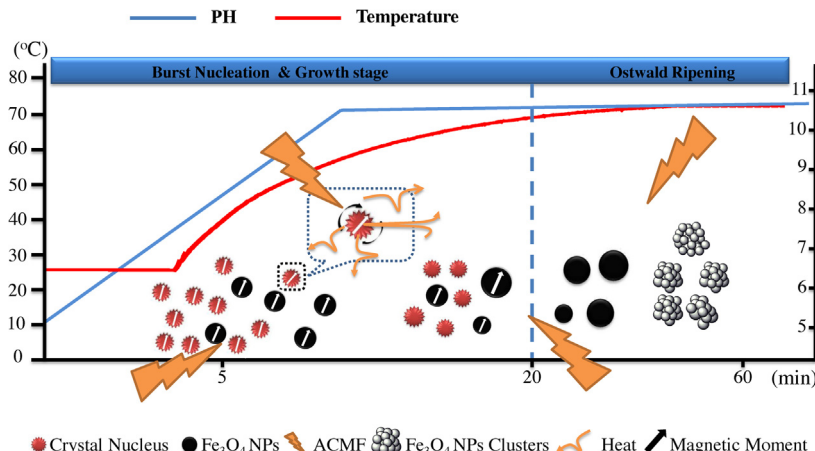
Yang Li<sup>1</sup>, Ke Hu<sup>1</sup>, Bo Chen, Yijun Liang, Fengguo Fan, Jianfei Sun, Yu Zhang, Ning Gu\*

State Key Laboratory of Bioelectronics, Jiangsu Laboratory for Biomaterials and Devices, School of Biological Sciences and Medical Engineering, Southeast University, Nanjing, China

## HIGHLIGHTS

- Fe<sub>3</sub>O<sub>4</sub> nanoparticle clusters with enhanced magnetic properties were prepared successfully by ACMF-assisted co-precipitation.
- The magnetic effect as well as heat effect of ACMF on Fe<sub>3</sub>O<sub>4</sub> nanoparticles plays a key role in the enhancement of magnetic properties during the whole synthesis process.
- This strategy might hold promise in preparation of high performance magnetic nanomaterials in the future.

## GRAPHICAL ABSTRACT



## ARTICLE INFO

### Article history:

Received 24 August 2016

Received in revised form 19 January 2017

Accepted 23 January 2017

Available online 24 January 2017

### Keywords:

Alternating-current magnetic field

Fe<sub>3</sub>O<sub>4</sub> nanoparticle clusters

Co-precipitation

Magnetism

Hyperthermia

## ABSTRACT

Field-assisted synthesis has been one of the common strategies of nanoparticles preparation with enhanced properties. However, most researches focused on exploring the effects of monofunctional static field on the structure and properties of synthetic nanomaterials, few researchers have applied fields with period variation as assistance. Combining medium alternating current magnetic field with most widely used method traditional chemical co-precipitation held potential in preparation high quality Fe<sub>3</sub>O<sub>4</sub> nanoparticle. In this study, Fe<sub>3</sub>O<sub>4</sub> nanoparticle clusters were prepared in alternating-current magnetic field (ACMF) by co-precipitation principle, structural and magnetic properties were also characterized. Results demonstrated that Fe<sub>3</sub>O<sub>4</sub> nanoparticle clusters prepared by co-precipitation heated in ACMF indicated a better heat production under ACMF, comparing with Fe<sub>3</sub>O<sub>4</sub> nanoparticle clusters with similar size and distribution prepared by classic co-precipitation. It might be due to the magnetic effects induced by ACMF that Fe<sub>3</sub>O<sub>4</sub> nanoparticles tend to grow along the magnetization direction. This technology might hold promise in preparation high performance magnetic nanomaterial in the future.

© 2017 Elsevier B.V. All rights reserved.

\* Corresponding author.

E-mail address: [guning@seu.edu.cn](mailto:guning@seu.edu.cn) (N. Gu).

<sup>1</sup> These authors contributed equally to this work and should be considered co-first authors.

## 1. Introduction

The effects of applied static field on the morphologies and properties of nanomaterial during the synthesis have been one of the hot spots for a long time [1]. Numerous researches paid attentions to the influence of static field on the dynamics and thermodynamics during the synthesis [2,3]. In addition, some similarly concentrated on rapid synthesis of magnetic nanoparticles on the assistance of time-varying field with high frequency, for example the microwave field [4,5]. Among the various fields, alternating-current magnetic fields (ACMF), especially ACMF with low or medium frequency, have been widely used in biomedical engineering areas [6]. Many works about magnetic inductive hyperthermia [7] and drug controlled release based on ACMF have been reported [8–10], which confirm that human body is tolerated by low or medium frequency ACMF. On account of this safety, nanomaterial with good biocompatibility and stability in body use for instance iron oxide nanoparticles could be prepared with assist of ACMF, yet few appeared.

As one of the most widely used magnetic nanomaterial in biomedical applications, iron oxide nanoparticles have been drawn attentions in many applications as bioseparation agent [11–13], drug carrier [14,15] and so on. The major advantages of well modified iron oxide nanoparticles is the good biocompatibility and stability. There are considerable iron oxide nanoparticles being approved and for clinical research. Ferumoxytol, a novel type of iron oxide nanoparticles, have been proved by USA Food and Drug Administration (FDA) as drugs for iron supplementation [6]. Besides, iron oxide nanoparticles with unique structures and characterizations could be fabricated with the assistance of applied static magnetic field [16,17].

As we all know, chemical co-precipitation process can well be explained by Lamer mechanism that a short burst of nucleation from a supersaturated solution and the slow growth of particles without any significant additional nucleation. And based on Brown relaxation and Néel relaxation theory [28], magnetic nanoparticles can produce heat accompanied with relaxation process of nanoparticles, in this procedure magnetic nanoparticles is magnetized and the magnetic moment is gradually arranged. In previous study [6], we have observed that the tiny particles after the initial nucleation can generate heat and increase reaction system temperature in the ACMF produced by moderate-radiofrequency heating machine, and have successfully prepared ferumoxytol, one kind of magnetic iron oxide nanomedicine with regular size and good magnetism.

In the meantime, we also found that PSC shows a prominent intervention effect on the nucleation and growth during the formation of iron oxide nanoparticles [18], so the iron core and hydrodynamic size of nanoparticle will be constrained as well as the magnetism, causing this nanoparticle inadequate in many applications e.g. magnetic hyperthermia. Herein, an alternative synthetic strategy developed for large size and high magnetic properties was finished. We aimed at adding PSC at the end of aging process in ACMF to alleviate the block effect,  $\text{Fe}_3\text{O}_4$  nanoparticle clusters with better magnetic properties could be formed instead of monodispersed nanoparticle. And the result showed comparing to nanoparticle clusters with similar size and dispersivity prepared by classic co-precipitation, this  $\text{Fe}_3\text{O}_4@\text{PSC}$  nanoparticle clusters indeed demonstrated higher saturation intensity and a better performance in heat generation in ACMF, which is great potential in magnetic hyperthermia.

## 2. Experimental

### 2.1. Materials and reagents

$\text{FeCl}_3 \cdot 6\text{H}_2\text{O}$  and  $\text{FeCl}_2 \cdot 4\text{H}_2\text{O}$  were purchased from Aladdin Chemical Reagent Company (Shanghai, China), 28% aqueous ammonia was from Lingfeng Chemical Reagent Company (Shang-

hai, China), Polydextrose sorbitol carboxyl methyl ether (PSC) was prepared from Jiangsu Key Laboratory for Biomaterials and Devices. All the chemical reagents were AR grade.

### 2.2. Fabrication of $\text{Fe}_3\text{O}_4$ nanoparticle clusters

To explore the difference in magnetic property between the nanoparticles clusters prepared by ACMF and those by oil bath, we firstly prepared samples by ordinary oil bath ( $70^\circ\text{C}$ ), and the amount of each material will be consistent with those of prepared in ACMF. we established an ordinary co-precipitation method after screening important factors in the reaction, confirmed each concrete parameter such as  $\text{Fe}^{3+}/\text{Fe}^{2+}$  ratio, the initial concentration of PSC and other steps followed by the traditional chemical co-precipitation principle. Then,  $\text{Fe}_3\text{O}_4$  nanoparticle clusters were fabricated in the ACMF and characterized for comparison with that prepared in classic method.

In brief, 0.74 mM of  $\text{FeCl}_3 \cdot 6\text{H}_2\text{O}$  and 0.5 mM of  $\text{FeCl}_2 \cdot 4\text{H}_2\text{O}$  were dissolved thoroughly in 5 ml of water in the round bottom plastic tube immobilized in the ACMF induction coil with a stirrer made of polytetrafluoroethylene and continuous nitrogen protection. The stirring speed was 600 rpm. Then 1 ml  $\text{NH}_4\text{OH}$  aqueous solution (5 mM/mL) was added dropwise to the reactor with the operation of the moderate radio frequency heating machine (Shuangping SPG-10-II, 340 KHz, 20 A, China) until the whole mixture became black, indicating the formation of  $\text{Fe}_3\text{O}_4$  nanoparticles. Then the reaction system was heated to  $70^\circ\text{C}$  and the output electric current of device was adjusted at 15A to maintain temperature, then aged for 40 min before the addition of 2 ml PSC aqueous solution (100 mg/mL). After that, the mixture was aged for another 15 min for unchanged temperature and output electric current. After it was cooled to room temperature, the nanoparticles was washed twice with ultrapure water to remove the redundant PSC,  $\text{Fe}^{2+}, \text{Fe}^{3+}, \text{NH}_4^+$  and  $\text{Cl}^-$ . The final products were collected through magnetic separation and dispersed in water. Moreover, another nanoparticle was obtained by ordinary co-precipitation method, and the materials and preparation process was the same with above steps except using oil bath as heat source.

### 2.3. Characterizations of $\text{Fe}_3\text{O}_4$ nanoparticle clusters

The morphology of the samples was examined by transmission electron microscope (TEM)(JEOL JEM-2100, Japan), The distribution state of nanoparticles clusters was characterized by Scanning electron microscope (SEM)(Zeiss, Ultra Plus, Germany), hydrodynamic diameter of the samples was measured by dynamic light scattering (DLS) (Malvern ZS-90, England), the crystal phase of samples was examined by x-ray powder diffraction with  $\text{Cu K}\alpha$  radiation on a X-ray diffractometer (Thermo X'TRA, USA) at room temperature. The magnetic properties ( $M$ - $H$  curve) of the samples were measured by Vibrating sample magnetometer (VSM) (Lakeshore 7407, USA). SAR evaluation of the sample dispersion (1 ml, 1 mg/mL Fe) was performed using an ACMF generator (Shuangping SPG-06-II, China) with the applied frequency was 390 KHz. The infrared thermal images of the samples was recorded by an Infrared Thermal Imager (Fluke Ti32, USA).

## 3. Results and discussion

The size and morphology will greatly affect the properties of nanomaterial [19,20]. Researches indicated that the single particle size would affect the heat generating under alternating magnetic field with different frequency [21]. TEM images indicated that by controlling the synthetic conditions, the single particle size of  $\text{Fe}_3\text{O}_4@\text{PSC}$  nanoparticle clusters prepared by alternating magnetic

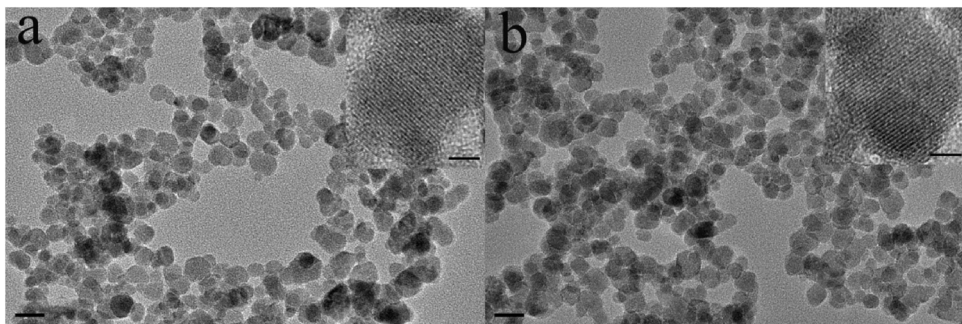


**Fig. 1.** TEM images of magnetic nanoparticle clusters prepared by alternating magnetic field assisted co-precipitation (a) and classic co-precipitation (b). Scale bar: 20 nm. HRTEM images of a single nanoparticle prepared by alternating magnetic field assisted co-precipitation (a) and classic co-precipitation (b). Scale bar: 5 nm.

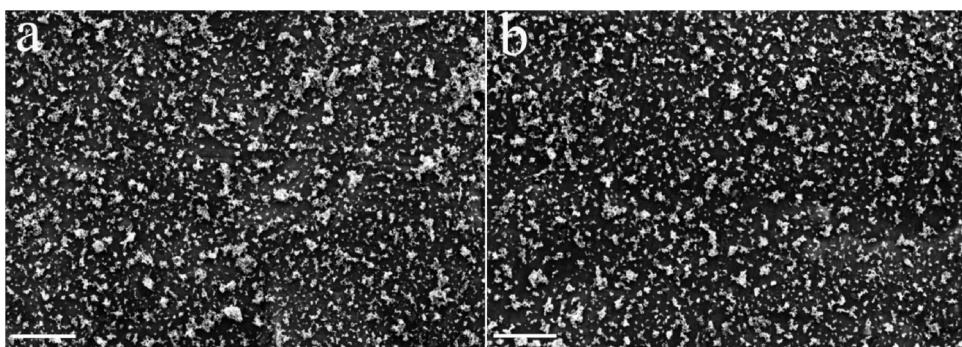


**Fig. 2.** SEM images of magnetic nanoparticle clusters prepared by alternating magnetic field assisted co-precipitation (a) and classic co-precipitation (b). Scale bar: 1  $\mu$ m.

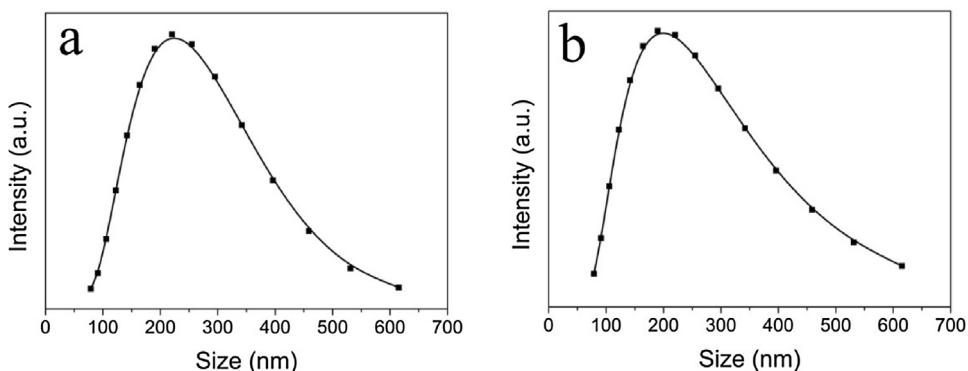


**Fig. 3.** DLS images of magnetic nanoparticle clusters prepared by alternating magnetic field assisted co-precipitation (a) and classic co-precipitation (b).

field assisted co-precipitation was  $12.7 \pm 1.2$  nm and the single particle size of  $\text{Fe}_3\text{O}_4@\text{PSC}$  nanoparticle clusters prepared by classic co-precipitation was  $12.5 \pm 1.6$  nm (Fig. 1), which were both close to the optimal size for hyperthermia under ACMF with medium frequency [21]. The high resolution TEM (HRTEM) images of a single nanoparticle prepared by ACMF assisted co-precipitation and classic co-precipitation showed the lattice spacing of 4.83 Å, which corresponded with the (111) plane of the cubic structure of  $\text{Fe}_3\text{O}_4$ . The selected area electron diffraction (SAED) was shown in Fig. S1. The presence of clear rings in Fig. S1 shows that the samples are all polycrystalline. Comparing to ferumoxytol synthesized in our previous work, the average size clearly increased. It was closely associated with the absence of PSC during the nucleation and growth of  $\text{Fe}_3\text{O}_4$ , which indulged the whole reaction process and leaded to the larger nanoparticles clusters [22].

Due to the high surface energy of unmodified magnetic nanoparticle prepared by co-precipitation, single nanoparticle intended to form large clusters. SEM images demonstrated that both sam-

ples were clusters composed of small nanoparticles (Fig. 2). The morphology of these nanoparticle clusters showed no obvious differences.

Hydrodynamic diameter obtained by DLS matched with the SEM and TEM results (Fig. 3). The hydrodynamic diameter of  $\text{Fe}_3\text{O}_4@\text{PSC}$  nanoparticle clusters prepared by alternating magnetic field assisted co-precipitation was  $208 \pm 58$  nm and the hydrodynamic radius of  $\text{Fe}_3\text{O}_4@\text{PSC}$  nanoparticle clusters prepared by classic co-precipitation was  $201 \pm 49$  nm. All these characterizations supported that the structures and morphologies of these magnetic nanoparticle clusters prepared by alternating magnetic field assisted co-precipitation and classic co-precipitation were of no great difference.

The crystal formation and degree of crystallinity are keys factors which influence saturation magnetization and heat generation properties of magnetic nanomaterial [23]. The peaks at  $18.3^\circ$ ,  $30.2^\circ$ ,  $35.6^\circ$ ,  $43.1^\circ$ ,  $53.3^\circ$ ,  $57.0^\circ$ ,  $62.4^\circ$  and  $75.0^\circ$  in XRD spectrum represented  $\text{Fe}_3\text{O}_4$  crystal plane 111, 220, 311, 400, 422, 511, 440, 622

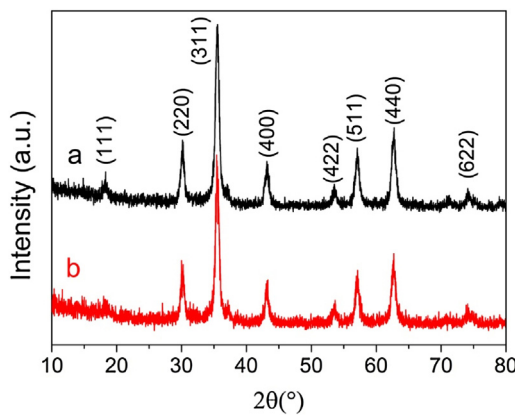


**Fig. 4.** XRD spectrum of magnetic nanoparticle clusters prepared by alternating magnetic field assisted co-precipitation (a) and classic co-precipitation (b).

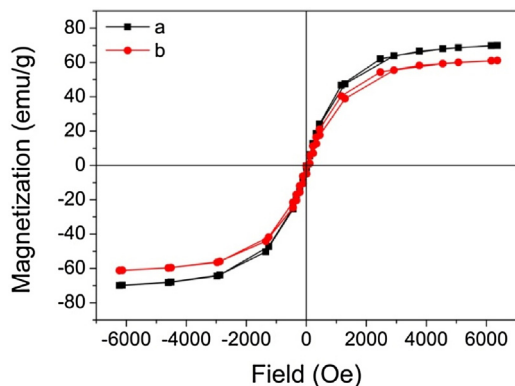


**Fig. 5.** VSM spectrum of magnetic nanoparticle clusters prepared by alternating magnetic field assisted co-precipitation (a) and classic co-precipitation (b).

respectively (Fig. 4). XRD results showed that samples prepared by ACMF assisted co-precipitation and classic co-precipitation were both  $\text{Fe}_3\text{O}_4$  nanoparticles. The crystal transformation from  $\text{Fe}_3\text{O}_4$  to  $\text{Fe}_2\text{O}_3$  could lead to the reduction of Saturation Magnetization, which would consequently give rise to the reduction of magnetic heat production capacity [24,25]. Thus compared with  $\text{Fe}_2\text{O}_3$  nanoparticles (e.g. ferumoxytol) prepared in our previous work, the  $\text{Fe}_3\text{O}_4$  nanoparticles clusters prepared in this study have better advantage in magnetic heat production capacity.

Saturation magnetization also plays an important role in altering the magnetothermal capability of nanomaterial. VSM was used to evaluate the magnetic properties of  $\text{Fe}_3\text{O}_4@\text{PSC}$  nanoparticle clusters prepared by ACMF assisted co-precipitation and classic

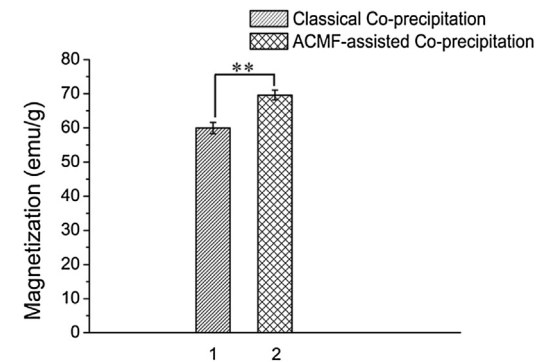


**Fig. 7.** Statistic data of magnetization of magnetic nanoparticle clusters prepared by classic co-precipitation(1) and alternating magnetic field assisted co-precipitation(2) ( $p = 4.82 \times 10^{-11} < 0.01$ ).

co-precipitation. Results indicated that the saturation intensity of  $\text{Fe}_3\text{O}_4@\text{PSC}$  nanoparticle clusters prepared by ACMF assisted co-precipitation was 69.2 emu/g, which was slightly larger than the saturation intensity (61.3 emu/g) of  $\text{Fe}_3\text{O}_4@\text{PSC}$  nanoparticle clusters prepared by classic co-precipitation with identical size (Fig. 5). Furthermore, the coercive force and residual magnetism of these nanomaterial were different. The coercive force and residual magnetism of  $\text{Fe}_3\text{O}_4@\text{PSC}$  nanoparticle clusters prepared by classic co-precipitation was circa 6 Oe and 0.3 emu/g respectively (Fig. 6a). However, the coercive force and residual magnetism of  $\text{Fe}_3\text{O}_4@\text{PSC}$  nanoparticle clusters prepared by alternating magnetic field assisted co-precipitation were circa thrice than those of  $\text{Fe}_3\text{O}_4@\text{PSC}$  nanoparticle clusters prepared by classic co-precipitation, which were 20 Oe and 1 emu/g accordingly (Fig. 6b). Statistic results based on ten different batch of  $\text{Fe}_3\text{O}_4@\text{PSC}$  nanoparticle clusters prepared by classic co-precipitation and alternating magnetic field assisted co-precipitation showed that the difference of magnetization between  $\text{Fe}_3\text{O}_4@\text{PSC}$  nanoparticle clusters prepared by classic co-precipitation and alternating magnetic field assisted co-precipitation were very significant (Fig. 7).

The magnetothermal effect of  $\text{Fe}_3\text{O}_4@\text{PSC}$  nanoparticle clusters prepared by ACMF assisted co-precipitation and classic co-precipitation were also characterized. Results showed that SAR of  $\text{Fe}_3\text{O}_4@\text{PSC}$  nanoparticle clusters prepared by alternating magnetic field assisted co-precipitation and classic co-precipitation were 402 and 345 W/g respectively (Fig. 8). The infrared thermal images indicated that the  $\text{Fe}_3\text{O}_4@\text{PSC}$  nanoparticle clusters prepared by alternating magnetic field assisted co-precipitation held potential as an agent of magnetic hyperthermia with good biocompatibility and high heating generation (Fig. 9).

Compared  $\text{Fe}_3\text{O}_4$  nanoparticles clusters obtained by ACMF with ordinary product, we can easily get the conclusion that the for-

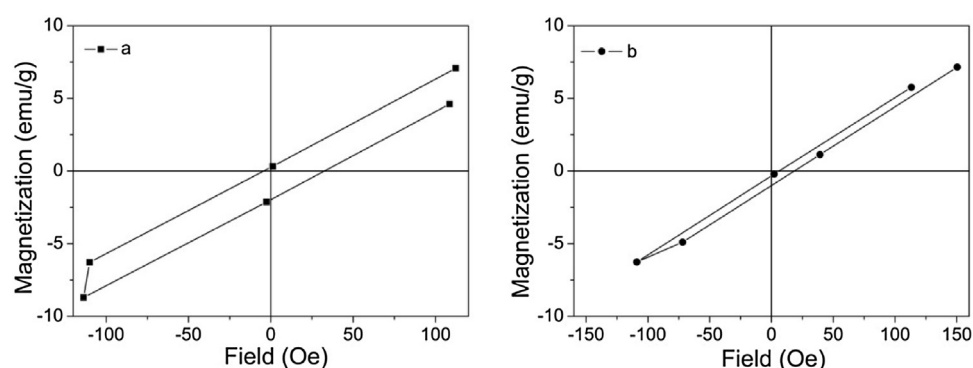


**Fig. 6.** Magnetic hysteresis loop of magnetic nanoparticle clusters prepared by alternating magnetic field assisted co-precipitation (a) and classic co-precipitation (b).

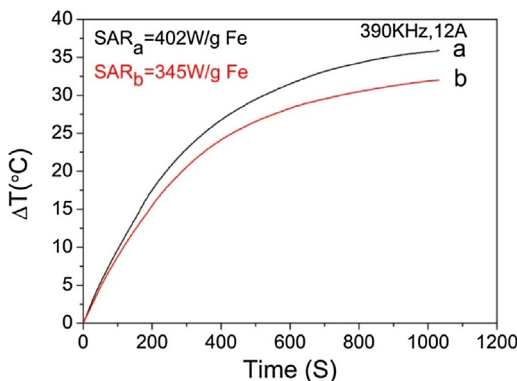


**Fig. 8.** Magnetothermal measurement of magnetic nanoparticle clusters prepared by alternating magnetic field assisted co-precipitation (a) and classic co-precipitation (b) under alternating magnetic field.

mer possess better magnetism. It is reported that FeOOH, the intermediate during the  $\text{Fe}_3\text{O}_4$  preparation in co-precipitation would be magnetized by static magnetic field with low intensity (0–250 Oe), which would affect the growth of iron oxide nanoparticles, inducing the growth along the axis of being easily magnetized and further be attributed to the improvement of magnetic properties [26,27]. And the similar phenomena occurred in the ACMF could be explained well according to this theory.

In view of the above speculations, we could deduce the possible process and mechanism, which was shown in Scheme 1. Initially, iron ion solution was added into alkali solutions at room temperature and a short burst of nucleation occurred followed Lamer mechanism. Moderate radio-frequency device started and ACMF was produced. After fast nucleation, the tiny iron oxide nuclear could generate heat through relaxation loss adhered to Brown

and Néel relaxation theory to make the solution temperature rise, meanwhile these smaller magnetized  $\text{Fe}_3\text{O}_4$  nuclear could grow slowly along the axis of being easily magnetized of biggish nanoparticles depending on the heat produced by themselves, during this procedure nuclear fused into bigger nanoparticle with the Ostwald Ripening. When the aging process ended, these particles grew to the size of approximately 10 nm and presented uniform size distribution confirmed by TEM Characterization (Fig. 1a). Lastly, PSC was mixed for coating on the surface of particles. PSC plays an important role in hinder effect and makes the particles stable existence in solution without bigger aggregates. After the coating step finished, iron oxide nanoparticle clusters of 12 nm in single iron core size formed because of high surface energy belongs to every nanoparticle and could be seen in SEM Characterization (Fig. 2a). These nanoparticle clusters demonstrated higher saturation magnetization intensity compared to ordinary  $\text{Fe}_3\text{O}_4$  nanoparticles prepared in oil bath, it may be concluded that  $\text{Fe}_3\text{O}_4$  nanoparticles tend to grow along the magnetization direction induced by ACMF.

#### 4. Conclusions

In conclusion, novel  $\text{Fe}_3\text{O}_4@\text{PSC}$  nanoparticle clusters were prepared in ACMF by co-precipitation. The magnetic properties and magnetothermal effect of  $\text{Fe}_3\text{O}_4@\text{PSC}$  nanoparticle clusters was studied and compared with  $\text{Fe}_3\text{O}_4@\text{PSC}$  nanoparticle clusters prepared by classic co-precipitation of similar size. As a result,  $\text{Fe}_3\text{O}_4@\text{PSC}$  nanoparticle clusters prepared in ACMF by co-precipitation displayed better saturation magnetization, coercive force, SAR and heating production under ACMF. As an explanation, the improvement in magnetic properties of samples prepared in ACMF might be due to the influence of ACMF on magnetic particle during the aging time, making nuclear tend to grow along magnetization direction to form nanoparticle with high magnetic

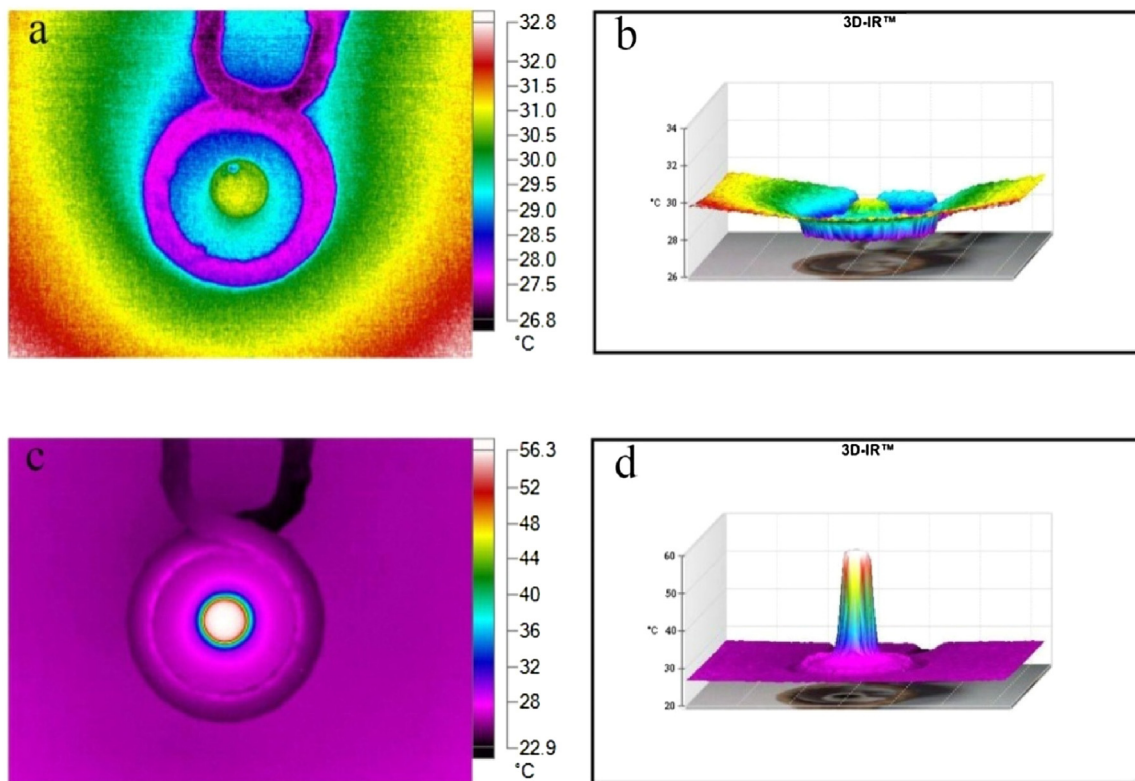
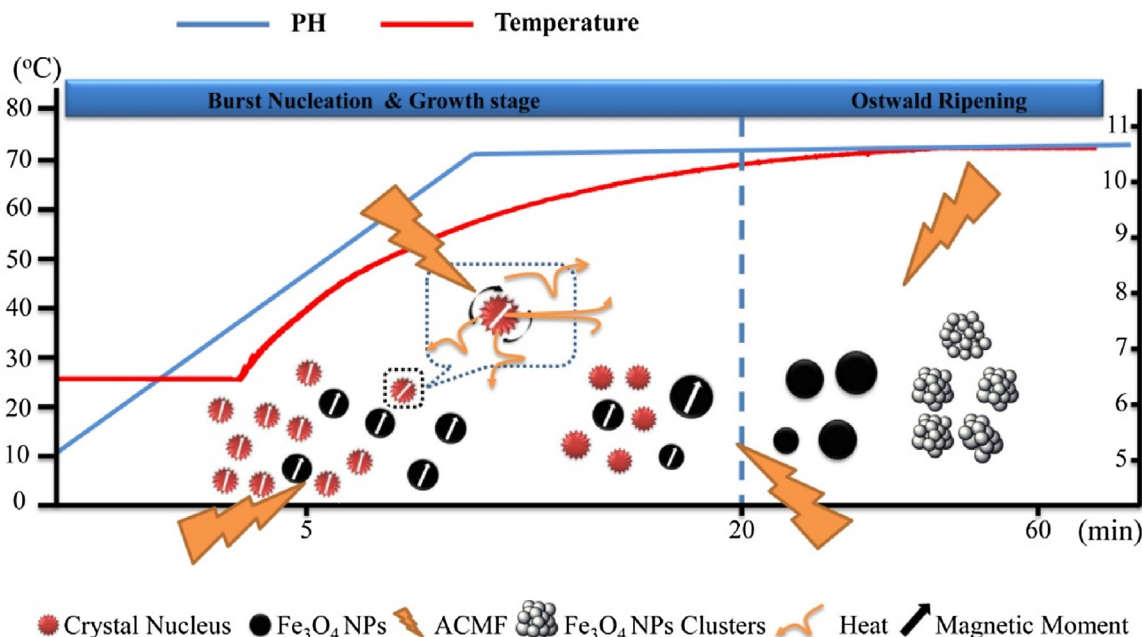


**Fig. 9.** Two dimensional and three dimensional infrared thermal images of magnetic nanoparticle clusters prepared by alternating magnetic field assisted co-precipitation before (a, b) and after applying ACMF for 10 min (c, d).



**Scheme 1.** Schematic illustration of preparation  $\text{Fe}_3\text{O}_4$  nanoparticle clusters induced by ACMF. The data include temperature controlled by an ACMF generator (SPG-10-II) and pH adjusted by  $\text{NH}_4\text{OH}$  aqueous solution.

properties. This strategy based on ACMF might hold promise in preparation high performance magnetic nanomaterial and for more extensive application.

## Acknowledgements

The authors gratefully acknowledge financial support from National Key Basic Research Program of China (2011CB933503, 2013CB733804), National Natural Science Foundation of China for Key Project of International Cooperation (61420106012), as well as National Natural Science Foundation of China (81473160). Thanks for the support from Collaborative Innovation Center of Suzhou Nano Science and Technology.

## Appendix A. Supplementary data

Supplementary data associated with this article can be found, in the online version, at <http://dx.doi.org/10.1016/j.colsurfa.2017.01.073>.

## References

- [1] J. Wang, Q. Chen, C. Zeng, B. Hou, Magnetic-field-induced growth of single-crystalline  $\text{Fe}_3\text{O}_4$  nanowires, *Adv. Mater.* 162 (2004) 137–140.
- [2] R. Hong, T. Pan, Y. Han, H. Li, J. Ding, S. Han, Magnetic field synthesis of  $\text{Fe}_3\text{O}_4$  nanoparticles used as a precursor of ferrofluids, *J. Magn. Magn. Mater.* 310 (2007) 37–47.
- [3] G. Nabiyouni, M. Julaee, D. Ghanbari, P.C. Aliabadi, N. Safaei, Room temperature synthesis and magnetic property studies of  $\text{Fe}_3\text{O}_4$  nanoparticles prepared by a simple precipitation method, *J. Ind. Eng. Chem.* 21 (2015) 599–603.
- [4] W. Xiao, X. Liu, X. Hong, Y. Lv, J. Fang, J. Ding, Magnetic-field-assisted synthesis of magnetite nanoparticles via thermal decomposition and their hyperthermia properties, *CrystEngComm* 17 (2015) 3652–3658.
- [5] I. Safarik, M. Safarikova, Magnetic techniques for the isolation and purification of proteins and peptides, *Biomagn. Res. Technol.* 2 (2004) 7–23.
- [6] J. Fan, J. Lu, R. Xu, R. Jiang, Y. Gao, Use of water-dispersible  $\text{Fe}_2\text{O}_3$  nanoparticles with narrow size distributions in isolating avidin, *J. Colloid Interface Sci.* 266 (2003) 215–218.
- [7] C. Xu, K. Xu, H. Gu, R. Zheng, H. Liu, X. Zhang, Z. Guo, B. Xu, Dopamine as a robust anchor to immobilize functional molecules on the iron oxide shell of magnetic nanoparticles, *J. Am. Chem. Soc.* 126 (2004) 9938–9939.
- [8] C. Alexiou, R.J. Schmid, R. Jurgens, M. Kremer, G. Wanner, C. Bergemann, E. Huenges, T. Nawroth, W. Arnold, F.G. Parak, Targeting cancer cells: magnetic nanoparticles as drug carriers, *Eur. Biophys. J.* 35 (2006) 446–450.
- [9] N. Kohler, C. Sun, A. Fichtenthaler, J. Gunn, C. Fang, M. Zhang, Methotrexate-immobilized poly(ethylene glycol) magnetic nanoparticles for MR imaging and drug delivery, *Small* 2 (2006) 785–792.
- [10] B. Chen, Y. Li, X. Zhang, F. Liu, Y. Liu, M. Ji, F. Xiong, N. Gu, An efficient synthesis of ferumoxylot induced by alternating-current magnetic field, *Mater. Lett.* 170 (2016) 93–96.
- [11] A. Osborne, E.M. Atkins, T.A. Gilbert, D.M. Kauzlarich, S.K. Liu, Rapid microwave-assisted synthesis of dextran-coated iron oxide nanoparticles for magnetic resonance imaging, *Nanotechnology* 23 (2012) 215602.
- [12] Z. Kozakova, I. Kuritka, E. Kazantseva, N. V. Babayan, M. Pastorek, M. Machovsky, P. Bazant, P. Saha, The formation mechanism of iron oxide nanoparticles within the microwave-assisted solvothermal synthesis and its correlation with the structural and magnetic properties, *Dalton Trans.* 44 (2015) 21099–21108.
- [13] G. Katsir, S.C. Baram, A.H. Parola, Effect of sinusoidally varying magnetic fields on cell proliferation and adenosine deaminase specific activity, *Bioelectromagnetic* 19 (1998) 46–52.
- [14] J. Xie, Y. Zhang, C. Yan, L. Song, S. Wen, F. Zang, G. Chen, Q. Ding, C. Yan, N. Gu, High-performance PEGylated Mn-Zn ferrite nanocrystals as a passive-targeted agent for magnetically induced cancer theranostics, *Biomaterials* 35 (2014) 9126–9136.
- [15] N.S. Singh, H. Kulkarni, L. Pradhan, D. Bahadur, A multifunctional biphasic suspension of mesoporous silica encapsulated with  $\text{YVO}_4:\text{Eu}^{3+}$  and  $\text{Fe}_3\text{O}_4$  nanoparticles synergistic effect towards cancer therapy and imaging, *Nanotechnology* 24 (2013) 065101.
- [16] K. Hu, J. Sun, Z. Guo, P. Wang, Q. Chen, M. Ma, N. Gu, A novel magnetic hydrogel with aligned magnetic colloidal assemblies showing controllable enhancement of magnetothermal effect in the presence of alternating magnetic field, *Adv. Mater.* 27 (2015) 2507–2514.
- [17] K. Hu, N. Zhou, Y. Li, S. Ma, Z. Guo, M. Cao, Q. Zhang, J. Sun, T. Zhang, N. Gu, Sliced magnetic polyacrylamide hydrogel with cell-adhesive microarray interface: a novel multicellular spheroid culturing platform, *ACS Appl. Mater. Interfaces* 8 (2016) 15113–15119.
- [18] S. Laurent, D. Forge, M. Prot, A. Roch, C. Robic, L.V. Elst, R.N. Muller, Magnetic iron oxide nanoparticles: synthesis, stabilization, vectorization physicochemical characterizations, and biological applications, *Chem. Rev.* 108 (2008) 2064–2110.
- [19] M. Ma, Y. Wu, J. Zhou, Y. Zhang, N. Gu, Size dependence of specific power absorption of  $\text{Fe}_3\text{O}_4$  particles in AC magnetic field, *J. Magn. Magn. Mater.* 268 (2004) 33–39.
- [20] M. Gonzales-Weimuller, M. Zeisberger, K.M. Krishnan, Size-dependant heating rates of iron oxide nanoparticles for magnetic fluid hyperthermia, *J. Magn. Magn. Mater.* 94 (2009) 7–50.
- [21] A.E. Deatsch, B.A. Evans, Heating efficiency in magnetic nanoparticle hyperthermia, *J. Magn. Magn. Mater.* 354 (2014) 163–172.

- [22] K. Tao, H. Dou, K. Sun, Combined investigation of experimental characterization and theoretic calculation on the structure of dextran- $\text{Fe}_3\text{O}_4$  clusters, *Colloids Surf A: Physicochem. Eng. Aspects* 290 (2006) 70–76.
- [23] R. Ghosh, L. Pradhan, Y.P. Devi, S.S. Meena, R. Tewari, A. Kumar, S. Sharma, N.S. Gajbhiye, R.K. Vatsa, B.N. Pandey, R.S. Ningthoujam, Induction heating studies of  $\text{Fe}_3\text{O}_4$  magnetic nanoparticles capped with oleic acid and polyethylene glycol for hyperthermia, *J. Mater. Chem.* 21 (2011) 13388–13398.
- [24] P. Saravanan, S. Alam, G.N. Mathur, Comparative study on the synthesis of  $\gamma\text{-Fe}_2\text{O}_3$  and  $\text{Fe}_3\text{O}_4$  nanocrystals using high-temperature solution-phase technique, *J. Mater. Sci. Lett.* 22 (2003) 1283–1285.
- [25] M. Aliahmad, N.N. Moghaddam, Synthesis of maghemite ( $\gamma\text{-Fe}_2\text{O}_3$ ) nanoparticles by thermal-decomposition of magnetite ( $\text{Fe}_3\text{O}_4$ ) nanoparticles, *Mater. Sci. Pol.* 31 (2013) 264–268.
- [26] L. Zhang, R. He, H. Gu, Synthesis and kinetic shape and size evolution of magnetite nanoparticles, *Mater. Res. Bull.* 41 (2006) 260–267.
- [27] Y. Zhou, *Modern Magnetic Materials Principle and Applications* (in Chinese), Chemical Industry Press, Beijing, 2002, pp. 306–309.
- [28] Xuman Wang, The heating effect of magnetic fluids in an alternating magnetic field, *J. Magn. Magn. Mater.* 293 (2005) 334–340.